$\mathcal{R}$esearch in
$\mathcal{A}$stronomy and
$\mathcal{A}$strophysics

Photometric analysis of two extreme low mass ratio contact binary systems

Surjit S. Wadhwa, Nick F. H. Tothill, Ain Y. DeHorta and Miroslav Filipović

School of Science, Western Sydney University, Locked Bag 1797, Penrith, NSW 2751, Australia;
19899347@student.westernsydney.edu.au

Abstract Multi-band photometry and light curve analysis for two newly recognized contact binary systems, TYC 6995–813–1 and NSVS 13602901, are presented. Both were found to be of extreme low mass ratios 0.11 and 0.17, respectively. The secondary components of both systems show evidence of considerable evolution with elevated densities as well as both luminosity and radii well above their main sequence counterparts. Even in the absence of significant spot activity, at least one of the systems, TYC 6995–813–1, displays features of magnetic and chromospheric activity. TYC 6995–813–1 is also determined to be a potential merger candidate with its current separation near the theoretical instability separation.

Key words: stars: binaries: eclipsing — stars: evolution — stars: low-mass — techniques: photometric

1 INTRODUCTION

A merger of contact binary star components is thought to result in a transient event referred to as a red nova. Estimates suggest that up to 1 in 500 stars in the Galaxy may be contact binaries (Rucinski 2007). A merger event is relatively rare and until recently there had been no confirmed observed events. The initial eruption of V1309 Scorpii (V1309 Sco) (Nakano et al. 2008) was thought to be a classical nova eruption because of the rapid increase in brightness. In the days following the initial eruption, V1309 Sco did not behave as expected, rapidly cooling in a matter of days (Mason et al. 2010). The spectrum became redder (cooler), as opposed to hotter as in a classical nova, suggesting the event was most likely a luminous red nova. Although not known prior to the event, the progenitor of V1309 Sco had been in the field of view of Optical Gravitational Lensing Experiment (OGLE) for a number of years prior to the outburst. Photometric analysis of the OGLE data indicated that the progenitor was indeed a contact binary system and that V1309 Sco was indeed a merger event between the components of a contact binary system with a resultant rapidly rotating single star (Tylenda et al. 2011). Recently there has been a rise in the interest of contact binary star mergers with a number of new projects exploring the theoretical (Wadhwa et al. 2021) and observational aspects (Gazeas et al. 2021)

There has been heightened interest in orbital stability of contact binary systems as a way of identifying potential merger candidates since the eruption of V-1309. The interplay of orbital and spin angular momentum is critical in maintaining orbital stability with instability likely if orbital angular momentum decreases below three times the total spin angular momentum of the components (Hut 1980). Determination of angular momentum is dependent on accurate determination of absolute parameters and contact binary systems provide one of the best avenues for determining the basic absolute parameters such as masses and radii of stars. Previous work (Arbutina 2007) has demonstrated that, in most instances, orbital instability is likely to occur in systems with extreme low mass ratios.

In this study, we report the multi-band photometry of two recently identified contact binary systems. We performed simultaneous multi-band analysis of the light curve using a recent version of the Wilson & Devinney (1971) code. We show that both systems are suitable for light curve analysis with complete eclipses, both are of extreme low mass ratio and both have significantly brighter and larger secondary components relative to their main sequence counterparts. In addition, where possible, we explore the evolution of the systems and other astrophysical indicators of potential instability.

2 PHOTOMETRY AND LIGHT CURVES

Images were acquired in B, V and R bands using the Western Sydney University (WSU) 0.6 m telescope equipped with an SBIG 8300T CCD camera and standard filters. Images were plate solved and differential photometry performed utilizing the American Association

of Variable Star Observers (AAVSO) VPHOT engine and differential photometry was also performed by relying on the VPHOT engine. The photometry report from the VPHOT engine gives an estimate of the error and all observations where the reported error exceeded 0.01 mag were excluded. We applied the method of Kwee & van Woerden (1956) to derive new times of minima and a new period was calculated utilizing the PSeach utility available through the AAVSO. The photometric data were folded using the derived period and times of minima. The deeper of the two eclipses was designated as the primary eclipse at phase zero. The maximum brightnesses for each pass-band at phase 0.25 and 0.75 were determined utilizing parabolic fit for observations from phases 0.24–0.26 and 0.74–0.76 respectively. In order to determine the absolute magnitude of the primary (see below), the V band magnitude at mid-secondary eclipse was taken as the average magnitude between phases 0.49–0.51 as all systems displayed a complete eclipse during this part of the phase cycle. A parabolic fit between phases 0.95 and 0.05 combined with the maximum magnitude was used to determine the amplitude of each system. As both systems being imaged are relatively new discoveries, no orbital period change analysis was possible given only scant (or nil) historical observations.

2.1 TYC 6995–813–1

TYC 6995–813–1 ($\alpha_{2000.0}$ = 00 06 49.98, $\delta_{2000.0}$ = −35 37 29.1) was identified as a contact binary both by the Catalina Sky Survey (Drake et al. 2017) and the All Sky Automated Survey for SuperNovae (ASAS-SN) (Jayasinghe et al. 2018) with a preliminary period of 0.38318 d. Differential photometry was performed with TYC 6995–815–1 as the comparison star and 2MASS 00071379-3534495 as the check star. The amplitude in V band was approximately 0.34 mag (12.08 – 12.42) while the difference between the primary and secondary eclipses, as expected, was small at 0.04 mag. The red band amplitude was 0.32 mag (11.97 – 12.29) while the blue band amplitude was 0.37 mag (12.63 – 13.00). The light curve demonstrates a complete eclipse lasting approximately 28 min. A single new minimum time for the primary eclipse was determined as HJD 2458797.9902 (0.0002) and a more refined period of 0.383130 (0.00002) d was calculated.

2.2 NSVS 13602901

NSVS 13602901 ($\alpha_{2000.0}$ = 16 46 09.83, $\delta_{2000.0}$ = −03 52 14.3) was recognized as a contact binary system both by the All Sky Automated Survey (Pojmanski 1997) and Northern Sky Variability Survey (Wozniak et al. 2003)

**Table 1** Light Curve Solution and Absolute Parameters for TYC 6995–813–1 and NSVS 13602901

| Parameter	TYC 6995–813–1	NSVS 13602901
Distance (pc)	498.0 ± 14	6114.4 ± 40
$M_1/M_\odot$	1.23 ± 0.01	1.19 ± 0.02
$M_2/M_\odot$	0.135 ± 0.01	0.203 ± 0.01
T_1(K) (Fixed)	6300	6250
T_2(K)	6235 ± 27	6222 ± 18
Inclination($^\circ$)	84.03 ± 1.51	83.59 ± 1.15
Fill-out(f)%	72 ± 2	44 ± 2
Potential(Ω)	1.941 ± 0.002	2.11 ± 0.007
r_1(mean)	0.633	0.554
r_2(mean)	0.288	0.260
Mass Ratio (M_2/M_1)	0.111 ± 0.002	0.171 ± 0.002
$A(R_\odot)$	2.46 ± 0.01	3.05 ± 0.01
$R_1/R_\odot$	1.46 ± 0.01	1.69 ± 0.01
$R_2/R_\odot$	0.60 ± 0.01	0.79 ± 0.01
$L_1/L_\odot$	2.29 ± 0.04	2.05 ± 0.04
$L_2/L_\odot$	0.73 ± 0.04	0.58 ± 0.02
Mv_1	3.93	4.05
Mv_2	5.17	5.42
R_1/R_{ZAMS}	1.37 ± 0.01	1.69 ± 0.01
R_2/R_{TAMS}	1.34 ± 0.01	1.31 ± 0.01
L_2/L_{TAMS}	314.7	61.9

with a preliminary period of 0.52379 d. Images of TYC 6995–813–1 were acquired using the UWS telescope and photometry was performed utilizing the VPHOT engine with TYC 5054-1601-1 as the comparison star and TYC 5058–642–1 as the check star. The V band amplitude was 0.4 mag (11.83 – 12.23) while difference in the eclipse depths was again 0.04 mag. The red band amplitude was 0.39 mag (11.47 – 11.86) while the blue band amplitude was 0.41 mag (12.45 – 12.86). The eclipses are complete, lasting approximately 69 min. A single new time for the primary minimum was determined as HJD 2458737.89608 (0.00003) while the period was refined to 0.5238905 (0.00002) d.

3 LIGHT CURVE ANALYSIS

Reliable light curve solutions of contact binary systems without spectroscopic mass ratios are only possible in cases where complete eclipses are present to constrain the highly correlated geometric parameters such as the mass ratio (q), inclination (i) and fill-out (f) (Terrell & Wilson 2005). Both our systems show complete eclipses and are thus suitable for photometric analysis without needing spectroscopic observations. All light curves were solved using a recent (2010) version of the Wilson-Devinney code (WD) (Wilson & Devinney 1971). As there was no appreciable variation in the two brightest magnitudes (O'Connell effect), only unspotted solutions were sought for both systems. As geometric elements account almost entirely for the shape of contact binary light curves (Rucinski 1993), certain parameters were fixed for both systems. As the components of contact binary systems are surrounded by a common envelope we
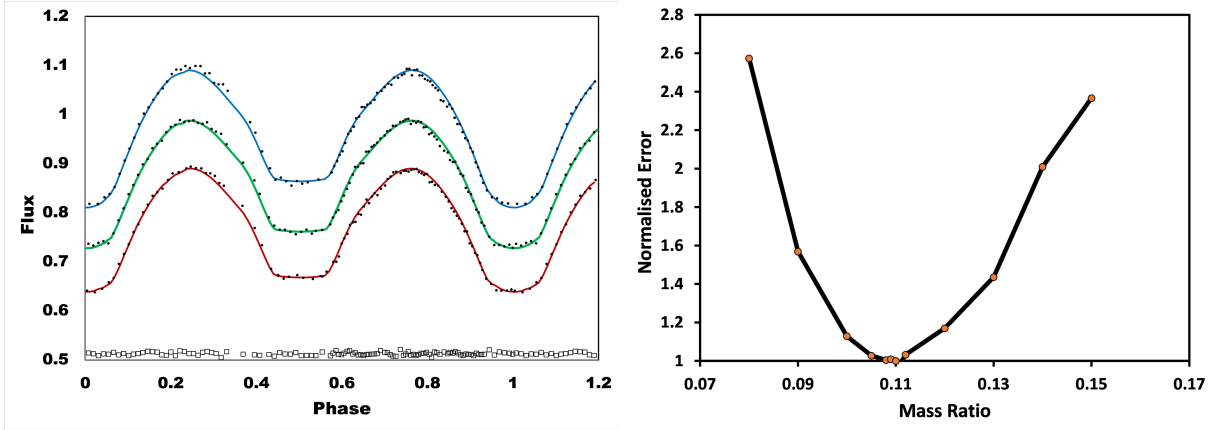
Fig. 1 Observed and fitted light curves (*left*) and mass ratio search grid (*right*) for TYC 6995–813–1. For ease of display, the *blue curves* are shifted up 0.1 units and the *red curves* shifted down 0.1 units. The check star flux displayed at the bottom of the light curve is shifted up by 0.1 units. The mass ratio search grid has been normalized to the minimum sum of the residuals (2.216×10^{-2}) as reported by the WD code.
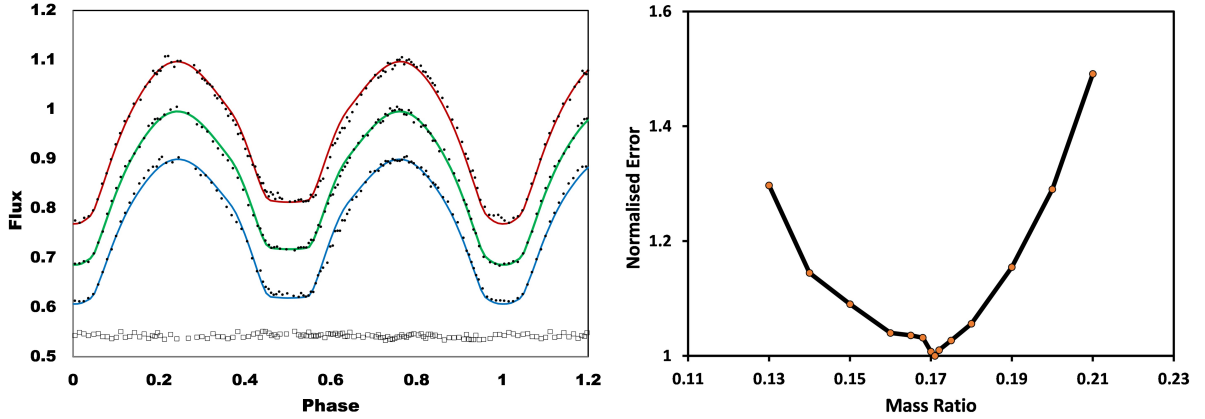
Fig. 2 Observed and fitted light curves (*left*) and mass ratio search grid (*left*) for NSVS 13602901. For ease of display, the *blue curves* are shifted up 0.1 unit and the *red curves* shifted down 0.1 units. The check star flux displayed at the bottom of the light curve is shifted down by 0.05 units. The mass ratio search grid has been normalized to the minimum sum of the residuals (3.51×10^{-1}) as reported by the WD code.

applied simple reflection treatment (Rucinski 1969) and fixed the bolometric albedos $A_1 = A_2 = 0.5$ and the gravity darkening coefficients $g_1 = g_2 = 0.32$ (Lucy 1967). Limb darkening coefficients for each pass-band were interpolated from van Hamme (1993) and logarithmic law applied as per Nelson & Robb (2015). The other fixed parameter in all cases was the effective temperature of the primary (T_1). This was estimated firstly by estimating the absolute magnitude of the primary (Mv_1) by considering the mid-eclipse magnitude (m) from the light curve (as this represents light from the primary only), distance (D) (Gaia Collaboration 2018) and interstellar reddening [$E(B-V)$] (Schlegel et al. 1998) as follows

$$M_v = m - (5 * \log_{10}(D/10)) + 3.1E(B-V). \quad (1)$$

Temperature of the primary was then determined from calibration for main sequence stars from Cox (2000).

There are various approaches to estimate the effective temperature of the primary with wide variations possible. In the case of NSVS 1360291, Gaia Collaboration (2018) reports the effective temperature as 5725 K while the LAMOST catalog (Luo et al. 2019) suggests the likely temperature of approximately 7300 K. As geometric parameters almost exclusively determine the shape of contact binary light curve variations in the estimate of T_1, this value will have no significant effect on the light curve solution with respect to the photometric mass ratio and other major parameters such as inclination and fill-out (Rucinski 1993).

Geometric parameters such as the mass ratio, inclination and degree of contact are the dominant variables determining the shape of contact binary light curves with gravity/limb darkening and reflection playing a minimal role (Rucinski 1993). As noted by Terrell & Wilson

(2005), significant correlation exists between the mass ratio and the other two major geometric parameters and reliable photometric solutions cannot be obtained, except in circumstances when a total eclipse occurs. The systematic mass ratio search grid method described by Russo & Sollazzo (1982) involves obtaining the best solution for a range of fixed values of the mass ratio q, with other parameters such as the temperature of the secondary (T_2), potential (fill-out) and inclination acting as free parameters. The solution with the smallest total error between the observed and modeled light curve is then selected as representing the true mass ratio. Terrell & Wilson (2005) previously demonstrated that such a technique when applied in cases of complete eclipses will yield the true mass ratio. For both systems, simultaneous multi-band solutions were obtained for various fixed incremental (0.01) values of q to initially find an approximate solution. Finer grid search at increments of 0.001 for the value of q was conducted near the approximate value to obtain the true mass ratio. In the final iteration, the mass ratio was also made a free parameter and the software reported standard deviations were recorded as the errors in the light curve solution. Fitted and observed light curves and mass ratio search grids for TYC 6995–813–1 and NSVS 13602901 are depicted in Figures 2.2 and 2.2 respectively while three-dimensional (3D) representations are illustrated in Figure 3. The light curve solution along with absolute and other astrophysical parameters (see below) are summarized in Table 1.

4 ABSOLUTE AND ASTROPHYSICAL PARAMETERS

Yildiz & Doğan (2013) showed that the primary components of contact binaries in terms of mass, radius and luminosity are much closer to those of normal zero age main sequence (ZAMS) stars than the secondary components. Despite their low masses, the secondary components are significantly brighter and larger than their ZAMS or terminal age main sequence (TAMS) counterparts. Using Equation (1) it is possible to determine the absolute magnitude of the primary and referencing the mass luminosity relation of Demircan & Kahraman (1991) and the light curve solution it is possible to determine the masses of both components. The error in the mass of the primary was estimated from the error in the distance (Gaia Collaboration 2018) and subsequent errors estimated through error propagation. As the total luminosity of the system is known and the luminosity of the primary is determined as described, the luminosity of the secondary can be easily derived. The hallmark of a contact binary system is that both components overflow their Roche lobes and as such their relative radii are dependent on the Roche

geometry and the mass ratio. As part of the light curve solution, the WD code provides the fractional radii of the component stars in three orientations. In this study, we use the geometric mean of the three directional radii as an estimate of the fractional radii of the primary (r_1) and secondary (r_2). From Kepler's third law, mass ratio and period it is possible to determine the separation (A) and from the separation the absolute radii of the components as per Awadalla & Hanna (2005), $R_{1,2} = Ar_{1,2}$, can be calculated.

Yildiz & Doğan (2013) compiled basic parameters for 100 well studied contact binary systems and showed good agreement between the luminosities of the primary component and main sequence stars of similar mass. With respect to the radii, they demonstrated that the primaries have somewhat larger radii than ZAMS stars. Unlike the primaries, the luminosities and radii of the secondaries do not correlate with main sequence stars of similar mass. They found that all secondary components were considerably brighter and larger than TAMS stars. The relative radii and luminosities and their relationship to ZAMS and TAMS are summarized in Table 1 and confirm the general reported findings.

Yildiz & Doğan (2013) argue that given the distorted nature of the secondaries, they must have different structure and evolutionary path relative to single stars. They assert that the interiors of the secondaries are quite different from those of main sequence stars because their initial mass was significantly higher than the present mass, as significant mass loss (or mass transfer) has occurred from the secondary to the primary. This situation means the present secondary component had a different evolutionary path compared to main sequence stars. Through detailed modeling, they showed that the present secondary was in fact larger and the initial primary lost mass to the initially smaller secondary through a semi-detached phase. The initial secondary grew larger while the initial primary grew smaller. Eventually, the initial secondary became larger than the mass losing primary and assumed the role of the present primary. Due to loss of mass from the outer layers of the current secondary, the internal structure of the current secondary is thought to be considerably denser than that of the primary. Modeling by Kähler (2004) indicated that the difference in the densities $\Delta\rho = \rho_1 - \rho_2$ ($\rho_{1,2}$ = densities of the primary and secondary respectively) is always negative for all contact binary systems. Knowing the period, radii, and mass ratio, the mean density of each component can be easily computed. The density (in $\mathrm{g\,cm^{-3}}$) of the components can be expressed as a function of the mass ratio, period and radii of the components (Mochnacki 1981) and the difference between the densities
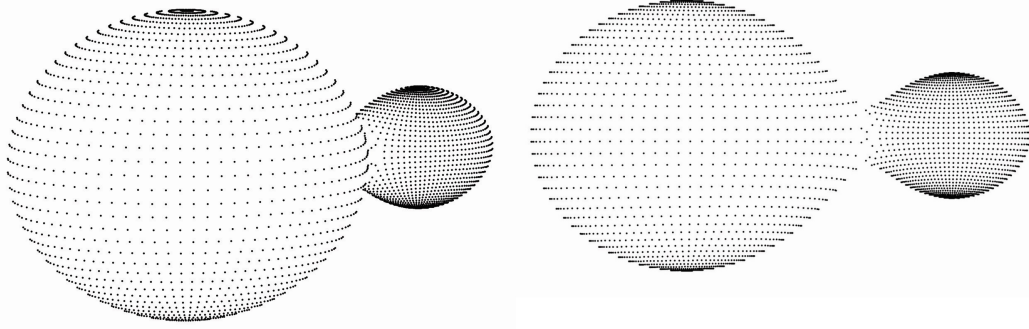
Fig. 3 3D representations of TYC 6995–813–1 (*left*) and NSVS 13602901 (*right*).

of the components can be written as follows

$$\Delta\rho = \frac{0.0189q}{R_2^3(1+q)P^2} - \frac{0.0189}{R_1^3(1+q)P^2}, \qquad (2)$$

where q is the current mass ratio, $R_{1,2}$ radii of the current primary and secondary and P is the period in days. $\Delta\rho$ was calculated for each of the systems and reported in Table 1. As predicted, it is strongly negative.

Contact binary systems are known to be magnetically active and hence potentially chromospherically active. Activity signals are common in contact binary systems. One of these is the asymmetry in the light curve maxima (O'Connell effect). Apart from star spot modeling, light curve analysis provides little indication of choromospheric activity although much clearer indicators such as certain emission lines are more specific for chromospheric activity. In the optical waveband, the chromospheric emissions are obscured by intense photospheric activity. The same however is not true for far ultraviolet (FUV) wavelengths, especially in the case of late type dwarfs which make up most contact binary systems (Smith & Redenbaugh 2010). The Galaxy Evolution Explorer (GALEX) satellite imaged the sky in two photometric band-passes: a near-ultraviolet band (NUV) with an effective wavelength of 2316 Å and an FUV band centered on 1539 Å (Morrissey et al. 2007). Only the FUV band is useful for the detection of chromospheric activity as the NUV band remains contaminated by photospheric activity (Smith & Redenbaugh 2010). A large volume of data on the strength of active chromospheric emission lines for a large number of late type dwarf stars exists as a result of the Mount Wilson HK project (Vaughan et al. 1978; Duncan et al. 1991). Smith & Redenbaugh (2010) used the GALEX FUV magnitudes (m_{FUV}) combined with the HK survey data to investigate the sensitivity of FUV brightness as an indicator of chromospheric activity.

The most accepted measure of chromospheric emission strength is the fraction of the star's bolometric luminosity emitted in the active H and K lines (Noyes et al. 1984). The value is normally expressed as $\log R'_{HK}$ and stars with $\log R'_{HK} \geq -4.75$ are considered more active (Henry et al. 1996). Utilizing the large database of $\log R'_{HK}$ values of dwarf stars, Smith & Redenbaugh (2010) matched the observations with GALEX magnitudes to derive a key relationship

$$(m_{\text{FUV}} - B)_{\text{base}} = 6.73(B - V) + 7.43, \qquad (3)$$

which defines the $m_{\text{FUV}} - B$ for stars with the weakest emissions and low activity. This is used as a correction term when defining the color excess

$$\Delta(m_{\text{FUV}} - B) = (m_{\text{FUV}} - B) - (m_{\text{FUV}} - B)_{\text{base}}. \quad (4)$$

They showed that for active stars, i.e. those with $\log R'_{HK} \geq -4.75$, the color excess was generally less than –0.5 and more frequently less than –1.0. Less active stars had color excess values significantly higher than –0.5. Only one of our systems, TYC 6995–813–1, was observed by GALEX with the reported m_{FUV} of 20.85. Using this and the relationships above (we rely on the published $B - V$ value from the ASAS-SN database) we derive the ultraviolet (UV) color excess of –2.89, indicating underlying significant chromospheric activity even in the absence of significant spot activity.

5 MERGER POTENTIAL

As noted above, contact binary systems are thought to merge when the orbital angular momentum falls below a critical (minimum) value. Recently, Wadhwa et al. (2021) demonstrated that orbital instability is not independent of the masses of the components but critically dependent particularly on the mass of the primary. They concluded that instability is unlikely unless the separation between the components was less than a critical value (A_{inst}) and showed that this could be expressed as a function of the mass ratio, radius of the primary and the gyration radii of the components, written as

$$\frac{A_{\text{inst}}}{R_1} = \frac{q\frac{k_2^2}{k_1^2}PQ + \sqrt{(q\frac{k_2^2}{k_1^2}PQ)^2 + 3(1 + q\frac{k_2^2}{k_1^2}Q^2)(q\frac{k_2^2}{k_1^2}P^2 + \frac{q}{(1+q)k_1^2})}}{q\frac{k_2^2}{k_1^2}P^2 + \frac{q}{(1+q)k_1^2}} \, . \tag{5}$$

Here $k_{1,2}$ is the gyration radius for the primary and secondary components and

$$P = \frac{0.49q^{2/3} - 3.26667q^{-2/3}(0.27q - 0.12q^{4/3})}{0.6q^{2/3} + \ln(1 + q^{1/3})} \, , \tag{6}$$

$$Q = \frac{(0.27q - 0.12q^{4/3})(0.6q^{-2/3} + \ln(1 + q^{-1/3}))}{0.15(0.6q^{2/3} + \ln(1 + q^{1/3}))} \, . \tag{7}$$

A review of the modeled values of the gyration radii (k) of low mass ($0.4\,M_\odot < M < 1.4\,M_\odot$) rotating and tidally distorted ZAMS stars by Landin et al. (2009) yields a simple linear relationship between the two as

$$k = -0.2455M + 0.5368 \, . \tag{8}$$

We use this relationship to derive the values of k_1 (gyration radius of the primary) for the two systems. The secondary is a very low mass star and for a low mass secondary, the convective n=1.5 polytrope is an excellent approximation (Arbutina 2007) for which $k_2 = 0.453$. This fixed value of k_2 and the variable value of k_1 from Equation (8) and absolute parameters derived above were adopted to calculate the instability separation, utilizing Equation (5), for both systems reported. The instability separation of TYC 6995–813–1 is estimated as $2.35\,R_\odot$ compared to the current separation only slightly higher at $2.46\,R_\odot$, suggesting the system is approaching instability. In contrast, the instability separation for NSVS 13602901 at $2.76\,R_\odot$ is significantly smaller than the current separation of $3.05\,R_\odot$, suggesting the system is likely to be stable.

6 SUMMARY AND CONCLUSIONS

The first multi-band photometric analysis of two bright southern contact binary systems is presented. We find both systems manifest extremely low mass ratios with evidence of significant age given the relative brightness, size and density of the "current" secondary relative to main sequence counterparts of similar mass. As expected, the primaries of both systems have absolute parameters not far removed from their ZAMS counterparts. Although neither system demonstrates a significant O'Connell effect, at least one of the systems that was observed by the GALEX mission does have features suggestive of significant chromospheric activity. Post V1309 Sco, orbital instability of contact binary systems has received considerable attention and at least one of our systems, TYC 6995–813–1, would fall into the category of being

a potential merger candidate. Among the most critical changes observed retrospectively for V1309 Sco was the exponential decline in its period in the years prior to the merger event (Tylenda et al. 2011). Given its relative brightness, TYC 6995–813–1 represents an easy target for long term follow up by smaller instruments such as campus telescopes or even advanced amateurs.

References

Arbutina, B. 2007, MNRAS, 377, 1635

Awadalla, N. S., & Hanna, M. A. 2005, Journal of Korean Astronomical Society, 38, 43

Cox, A. N. 2000, Allen's Astrophysical Quantities (AIP)

Demircan, O., & Kahraman, G. 1991, Ap&SS, 181, 313

Drake, A. J., Djorgovski, S. G., Catelan, M., et al. 2017, MNRAS, 469, 3688

Duncan, D. K., Vaughan, A. H., Wilson, O. C., et al. 1991, ApJS, 76, 383

Gaia Collaboration 2018, VizieR Online Data Catalog, I/345

Gazeas, K. D., Loukaidou, G. A., Niarchos, P. G., et al. 2021, MNRAS, 502, 2879

Henry, T. J., Soderblom, D. R., Donahue, R. A., & Baliunas, S. L. 1996, AJ, 111, 439

Hut, P. 1980, A&A, 92, 167

Jayasinghe, T., Kochanek, C. S., Stanek, K. Z., et al. 2018, MNRAS, 477, 3145

Kähler, H. 2004, A&A, 414, 317

Kwee, K. K., & van Woerden, H. 1956, Bull. Astron. Inst. Netherlands, 12, 327

Landin, N. R., Mendes, L. T. S., & Vaz, L. P. R. 2009, A&A, 494, 209

Lucy, L. B. 1967, ZAp, 65, 89

Luo, A. L., Zhao, Y. H., Zhao, G., & et al. 2019, VizieR Online Data Catalog, V/164

Mason, E., Diaz, M., Williams, R. E., Preston, G., & Bensby, T. 2010, A&A, 516, A108

Mochnacki, S. W. 1981, ApJ, 245, 650

Morrissey, P., Conrow, T., Barlow, T. A., et al. 2007, ApJS, 173, 682

Nakano, S., Nishiyama, K., Kabashima, F., et al. 2008, IAU Circ., 8972, 1

Nelson, R. H., & Robb, R. M. 2015, Information Bulletin on Variable Stars, 6134, 1

Noyes, R. W., Hartmann, L. W., Baliunas, S. L., et al. 1984, ApJ, 279, 763

Pojmanski, G. 1997, Acta Astronomica, 47, 467

Rucinski, S. 1969, Postepy Astronomii Krakow, 17, 163

Rucinski, S. M. 1993, PASP, 105, 1433

Rucinski, S. M. 2007, MNRAS, 382, 393

Russo, G., & Sollazzo, C. 1982, A&A, 107, 197

Schlegel, D. J., Finkbeiner, D. P., & Davis, M. 1998, ApJ, 500, 525

Smith, G. H., & Redenbaugh, A. K. 2010, PASP, 122, 1303

Terrell, D., & Wilson, R. E. 2005, Ap&SS, 296, 221

Tylenda, R., Hajduk, M., Kamiński, T., et al. 2011, A&A, 528, A114

van Hamme, W. 1993, AJ, 106, 2096

Vaughan, A. H., Preston, G. W., & Wilson, O. C. 1978, PASP, 90, 267

Wadhwa, S. S., De Horta, A., Filipović, M. D., et al. 2021, MNRAS, 501, 229

Wilson, R. E., & Devinney, E. J. 1971, ApJ, 166, 605

Wozniak, P. R., Vestrand, W. T., McGowan, K. E., et al. 2003, in American Astronomical Society Meeting Abstracts, 203, 57.03

Yildiz, M., & Doğan, T. 2013, MNRAS, 430, 2029